Available online at www.sciencedirect.com
SCIENCE DIRECT®

C. R. Chimie 7 (2004) 725–736

COMPTES RENDUS
CHIMIE

Full paper / Mémoire

Surface organometallic chemistry: a route to well-defined boron heterogeneous co-catalyst for olefin polymerisation

Nicolas Millot, Catherine C. Santini *, Frédéric Lefebvre, Jean-Marie Basset

Laboratoire de chimie organométallique de surface, UMR 9986 CNRS–ESCPE Lyon,
43, bd du 11-Novembre-1918, 69626 Villeurbanne cedex, France

Received 14 November 2003; accepted 11 March 2004

Abstract

The reaction of tris(pentafluorophenyl)borane, $B(C_6F_5)_3$ with surface silanol (≡Si–OH) of silica occurs *only* in the presence of a Brønsted base (diethylaniline, Et_2NPh), which does not form a complex with $B(C_6F_5)_3$, and affords selectively a well-defined ionic entity $[\equiv SiO{-}B(C_6F_5)_3]^-[HNEt_2Ph]^+$. With a strong nucleophile base such as pyridine (C_5H_5N), the complex $(C_6F_5)_3B.NC_5H_5$ is formed and is only physisorbed onto silica surface. Without a base, $B(C_6F_5)_3$ does not react with (≡Si–OH), and is only physisorbed. On the contrary, with any molecular compound ROH, $B(C_6F_5)_3$ forms a stable complex $(C_6F_5)_3B{\cdot}O(H)R$. ***To cite this article: N. Millot et al., C. R. Chimie 7 (2004).***

Résumé

Le tris(pentafluorophényl)bore $B(C_6F_5)_3$ ne réagit avec les groupes silanol (≡Si–OH) de surface de la silice qu'en présence d'une base de Brønsted (diéthylaniline, Et_2NPh), qui, ne formant pas de complexe avec $B(C_6F_5)_3$, conduit de façon sélective à une entité ionique de surface $[\equiv SiO{-}B(C_6F_5)_3]^-[HNEt_2Ph]^+$ bien définie. Avec une base plus nucléophile telle que la pyridine (C_5H_5N), il y a formation du complexe $(C_6F_5)_3B.NC_5H_5$ qui est seulement physisorbé sur la surface de silice. En l'absence de base, $B(C_6F_5)_3$ est simplement physisorbé de façon réversible sur la surface de silice, alors qu'il forme avec tout dérivé moléculaire ROH un complexe stable $(C_6F_5)_3B{\cdot}O(H)R$. ***Pour citer cet article : N. Millot et al., C. R. Chimie 7 (2004).***

Keywords: Tris(pentafluorophenyl)borane; Silica; Diethylaniline; Heterogeneous anions; Polymerisation co-catalyst

Mots clés : Tris(pentafluorophényl)borane ; Silice ; Diéthylaniline ; Anions hétérogénes ; Co-catalyseur de polymérisation

---

* Corresponding author.
E-mail address: santini@cpe.fr (C.C. Santini).

doi:10.1016/j.crci.2004.03.011

1. Introduction

One of the most exciting developments in the areas of catalysis, organometallic chemistry, and polymer science in recent years has been the new polymerisation technologies based on single-site and metallocene coordination olefin polymerisation catalysts [1,2]. The vast number of specifically designed/synthesized transition metal complexes (catalyst precursors) and main-group organometallic compounds (co-catalysts) allows unprecedented control over polymer microstructure, the generation of new polymer architectures, and the development of new polymerisation reactions. A large proportion of commercial polyolefin production is currently achieved by large-scale slurry- and gas-phase polymerisation processes, which require the polymerisation catalysts to be anchored on solid supports. Although supported catalysts are generally less active than homogeneous catalysts, they often offer advantages in producing polymeric products with good morphology and high bulk density. In these supported catalysts, grafted main-group organometallic fragments (co-catalysts) could act as heterogeneous anions on which the metallocenium species are stabilized by ion-pair interactions [2,3] (Scheme 1). Generally, the intimate structure of the active site(s) remains unknown.

Since two decades, the surface organometallic chemistry (SOMC) principle allows to develop access to unique and well-defined organometallic fragments linked to the silica surface [4]. The focus of this paper is to access to a well-defined boron heterogeneous co-catalyst using this approach, in the case of the reaction of tris(pentafluorophenyl)borane, $B(C_6F_5)_3$ with the silica surface in presence or not of Brønsted bases.

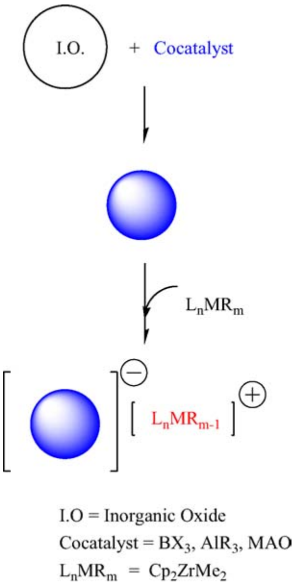

Scheme 1.

2. Results

Interestingly, although the synthesis of tris(pentafluorophenyl)boron, $B(C_6F_5)_3$, was known since 1963 [5], very few reports appeared until recently on the reaction of this non-hydrolysable Lewis acid with silica surfaces [6–10]. An attractive feature could be the ability of $B(C_6F_5)_3$ to enhance the Brønsted acidity of silica by reversible coordination with the surface hydroxyl groups (Eq. (1)) [8]. This behaviour has been observed in solution with Lewis bases such as water [11–16] alcohols [11,16] and silanols [17]. However, the lack of spectroscopic evidences supporting reaction (1) in the solid state justified a more systematic approach, which will be the aim of the first part of this work.

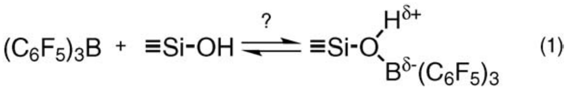

$$(C_6F_5)_3B \;+\; \equiv Si\text{-}OH \overset{?}{\rightleftharpoons} \equiv Si\text{-}O(H^{\delta+})B^{\delta-}(C_6F_5)_3 \qquad (1)$$

In the second part, the results of the reaction of $B(C_6F_5)_3$ with silica in the presence of a Brønsted base (C_5H_5N and Et_2NPh) will be reported.

In both cases, the fully characterization by infrared and multinuclear (^1H, ^{13}C, ^{11}B) solid-state NMR spectroscopy, elemental analysis, labelling, chemical reactivity, molecular modelling and synthesis of molecular analogues will be described.

2.1. Silica surface

Among the large variety of accessible oxide supports, silica is probably the simplest and the best understood. Its surface is composed of relatively unreactive (at least for moderate temperatures of dehydroxylation) siloxane bridges ≡Si–O–Si≡, and surface hydroxyl groups ≡Si–OH. A huge amount of vibrational spectroscopy and solid-state NMR (^{1}H, ^{29}Si) studies have largely contributed to the determination, the distribution and the reactivity of these surface reactive sites. Some recent reviews are particularly interesting in this field [18–20]. The design of single-site supported organometallic complexes requires the perfect knowledge and the precise control of the surface reactive sites. Their nature and concentration are indeed strongly determining in the final structure of the surface organometallic fragments. A preliminary study of the surface morphology as a function of the pretreatment temperature is then essential prior to chemical modification.

The support used for our studies was a pyrogenic (Degussa Aerosil© 200). The specific area was 200 m^2 g^{-1} for $SiO_{2-(300,500)}$, 180 m^2 g^{-1} for $SiO_{2-(700,800)}$ and 160 m^2 g^{-1} for $SiO_{2-(1000)}$. The influence of the dehydroxylation temperature on the nature and of the proportion of the reactive surface sites was studied by infrared and ^{1}H NMR spectroscopies.

The dehydroxylation of a compacted silica disk (10 mg) under vacuum was followed by infrared spectroscopy for temperatures ranging from 25 to 1000°C. The overall effect was an increase in the number of isolated silanol groups and an increase in the intensity of the 3747-cm^{-1} IR band. The consumption of the H-bonded silanols was complete above 500 °C, and only isolated and terminal silanols at 3747 and 3720 cm^{-1} were still observed at this temperature. For dehydroxylation temperatures above 500 °C, the low wavenumber asymmetry of the residual isolated silanol peak at 3747 cm^{-1} disappeared and the band became narrower and more symmetrical. For the silica used in our studies, a qualitative approach was carried out by measuring the areas of each type of silanols (bridged and/or isolated) as a function of the dehydroxylation temperatures (Fig. 1). H-bonded silanols represented the majority of the surface hydroxyl groups initially present on silica. As the dehydroxylation temperatures increased, the sum of all silanols (▲) decreased in a same manner than that of bridged silanols (■). Due to the condensation of bridged silanols, the amount of isolated silanols (♦) increased and reached a maximum between 300–400 °C. For higher temperatures (≥ 500 °C), the condensation of isolated silanols occurred and their proportion decreased. At 600 °C, there was no more bridged silanols on the surface. However, since the extinction coefficients of each ν(O–H) vibration have not been calibrated, the relative quantification of the surface silanols by infrared was not possible.

Solid-state ^{1}H NMR spectra of silica samples dehydroxylated at temperatures below 500 °C displayed two peaks at 2.7 and 1.8 ppm. These peaks were respectively assigned to H-bonded, and isolated/geminal surface silanols. Isolated and geminal hydroxyl groups cannot be differentiated by solid-state ^{1}H NMR spectroscopy (the existence of geminal silanols was only evidenced by ^{29}Si NMR spectroscopy [21-23]. For dehydroxylation temperatures above 500 °C, the persistence of the sharp peak at 1.8 ppm demonstrated that only isolated silanols were present on the surface, as shown previously by infrared spectroscopy.

In NMR spectroscopy, the intensity of a signal is directly proportional to the total number of spins present in the sample. Then, relative intensities can be obtained from relative areas of resonance lines, and absolute intensities, from comparison with an external standard. For silica samples, the signals observed for isolated (1.8 ppm) or H-bonded (2.7 ppm) hydroxyls in ^{1}H NMR spectra are therefore proportional to the total amount of surface silanols, this latter being dependant on the mass of the samples and on the pre-treatment temperature. The peaks areas, divided by the mass of the corresponding samples, are representative of the total amount of surface silanols for a given dehydroxylation temperature. Solid-state ^{1}H NMR spectroscopy was then used to quantify the surface silanols for silica dehydroxylated at various temperatures, by reference to NH_4Cl as an external standard. The surface concen-

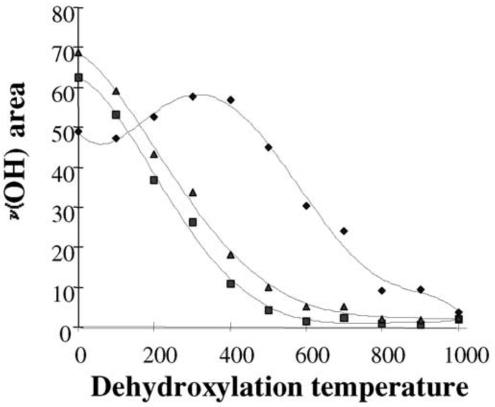

Fig. 1. Infrared areas of the ν(OH) vibrations versus dehydroxylation temperatures for (■) bridged silanols, (♦) isolated silanols and (▲) sum of all silanols.

Table 1
Experimental data and results for the quantification of surface silanols by solid-state ^1H NMR spectroscopy

Sample	T (°C)	Time (h) [a]	Weight (mg)	Intensity I [b]	RG[c]	Intensity/g (RG = 100)[d]	δ_{OH} mmol g^{-1}[e]	α_{OH} (OH nm^{-2})[f]
NH_4Cl	—	—	48.5	713	64	23000	74.8	—
$SiO_{2\text{-}(150)}$	150	14	19.9	112	2048	275	0.894	2.69
$SiO_{2\text{-}(200)}$	200	13	24.3	119	2048	239	0.778	2.35
$SiO_{2\text{-}(300)}$	300	14	28.0	101	2048	176	0.572	1.72
$SiO_{2\text{-}(350)}$	350	8	27.0	162	4096	146	0.476	1.43
$SiO_{2\text{-}(400)}$	400	14	27.9	145	4096	127	0.413	1.24
$SiO_{2\text{-}(500)}$	500	10	35.2	176	4096	123	0.40	1.2
$SiO_{2\text{-}(800)}$	800	13	35.9	100	4096	68	0.223	0.6
$SiO_{2\text{-}(1000)}$	1000	14	37.0	58	4096	40	0.132	0.4

[a] Dehydroxylation time at a given temperature.

[b] Integration on the [(+20)–(–20) ppm] interval.

[c] Sensitivity factor.

[d] Intensity/weight reported to a RG value of 100.

[e] For NH_4Cl: calculated on the basis that 1 g of NH_4Cl contains 74.8 mmol of hydrogen; for $SiO_{2\text{–}(T)}$: (I/g – $SiO_{2\text{-}(T)}$) × ($mmol_H$ g^{-1} – NH_4Cl)/(I/g – NH_4Cl).

[f] With specific areas of 200 m^2 g^{-1} for $SiO_{2\text{–}(150\text{–}500)}$, 180 m^2 g^{-1} for $SiO_{2\text{–}(800)}$ and 160 m^2 g^{-1} for $SiO_{2\text{–}(1000)}$.

tration α_{OH} of hydroxyl groups (OH/nm^2) was then deduced from these data and the surface area as measured by nitrogen adsorption (Table 1).

It can be noted that the two analytical methods (^1H NMR and TGA) used for Aerosil silica were bulk methods measuring all OH groups, including internal and reactively inaccessible silanol groups. In conclusion, infrared spectroscopy brought qualitative aspects on the evolution and the distribution of surface reactive sites during the condensation process. Solid-state ^1H NMR allowed the quantification of all hydroxyl groups present on silica.

2.2. Reactivity of $B(C_6F_5)_3$ with silica surface

A large excess (5 equiv) of $B(C_6F_5)_3$ was reacted in toluene with $SiO_{2\text{–}(500,700,1000)}$ for 2 h, at room temperature. The resulting pink solids were washed three times with toluene {these washings were collected for further analyses}and dried to give light pink ($SiO_{2\text{–}(500,700)}$) or white ($SiO_{2\text{–}(1000)}$) solids, **1**.

The results of elemental analyses revealed a general loading of 0.1–0.2 w% of boron, which corresponds to a concentration of around 0.6 boron per surface silanol. After toluene washings, elemental analyses showed that 30 to 60% of boron has leached. This proved that only weak interactions were involved between $B(C_6F_5)_3$ and the silica surface (Table 2).

IR spectra of solids **1**, the bands characteristic of the starting material at 1650, 1523, 1470, 1380 (C_6F_5 groups[16,24,25] and 1325 $cm^{-1}$are present (Fig. 2).

The most significant result was that in these spectra, (Fig. 2), the position and the intensity of the band due to the vibration of the free silanol, ν(≡Si–OH), at 3748 cm^{-1} was identical before and after reaction with $B(C_6F_5)_3$. What is more, the ^{19}F NMR spectra of the toluene filtrate (washings) of solids **1** showed only peaks at –129, –142 and –160 ppm, which were unambiguously attributed to ortho-, para- and meta-fluorine atoms of pure $B(C_6F_5)_3$. No C_6F_5H was detected by ^{19}F NMR spectroscopy and gas chromatography in the filtrate solution. Likewise, the ^1H NMR spectrum of

Table 2
Results of elemental analysis for **1** in function of the dehydroxylation temperature of the silica and the workup

Runs	T (°C)	OH (nm^2)	Before washing		After washing	
			% B [a]	B/OH [b]	% B [a]	B/OH [b]
1	500	1.2	0.33	0.54	0.23	0.38
2	700	0.7	0.24	0.70	0.10	0.29

[a] Weight %.

[b] Calculated from molar % of B.

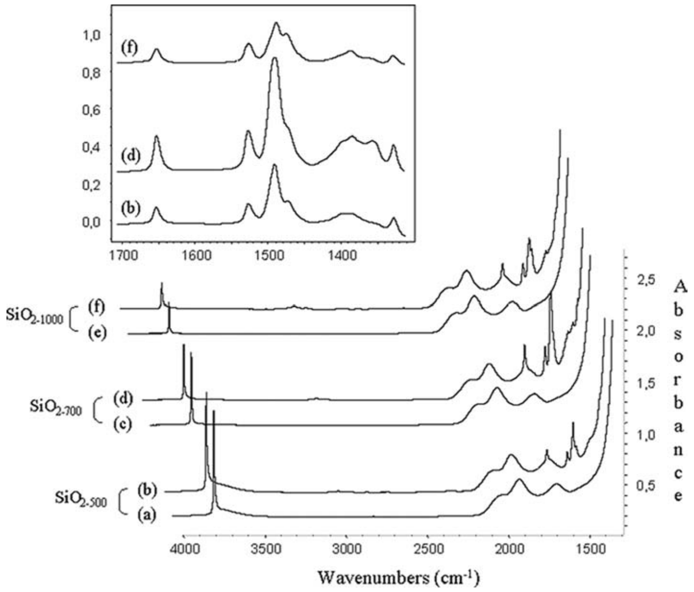

Fig. 2. IR spectra of (**a**) $SiO_{2-(500)}$; (**b**) $SiO_{2-(500)}$ after reaction with $B(C_6F_5)_3$ (5 equiv) in toluene; (**c**) $SiO_{2-(700)}$; (**d**) $SiO_{2-(700)}$ after reaction with $B(C_6F_5)_3$ (5 equiv) in toluene; (**e**) $SiO_{2-(1000)}$; (**f**) $SiO_{2-(1000)}$ after reaction with $B(C_6F_5)_3$ (5 equiv) in toluene; and expanded 3800–3200 cm^{-1} region.

solids **1** revealed no significant difference in chemical shifts of surface isolated silanol groups ≡Si–OH. ($\Delta\delta$ = 0.1 ppm) as expected if the surface Brønsted acidity has been created by interaction of $B(C_6F_5)_3$ with them [26]. These results indicated that the $B–C_6F_5$ bond was not cleaved (Eq. (2)), that there was no interaction of any type between $B(C_6F_5)_3$ and the oxygen atom of ≡Si–OH (Eq. (3)), and that $B(C_6F_5)_3$ was only physisorbed onto the silica surface (Eq. (4)).

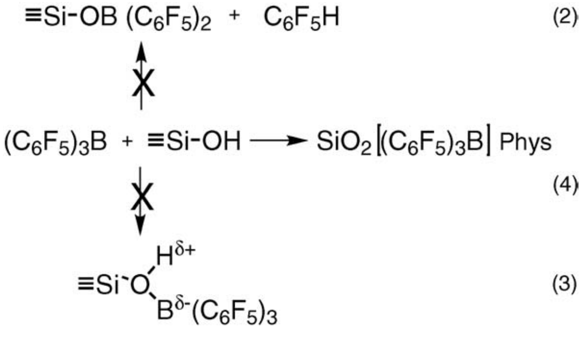

In order to model the reaction of $B(C_6F_5)_3$ with silica surfaces, the reactivity of equimolar amounts $B(C_6F_5)_3$ and R–OH compounds (R = H, Ph_3Si, (*c*-$C_5H_9)_7O_{12}Si_8$) in benzene, at room temperature, was investigated by solution ^1H, ^{13}C, ^{19}F and ^{11}B NMR spectroscopy. ^{19}F NMR spectra recorded for these solutions showed a general upfield shift of the para-fluorine after reaction with R–OH (Table 3). Such a shift was characteristic of a change in the boron geometry from trigonal to tetrahedral, induced by coordination with the hydroxy oxygen atom. The difference $\Delta(\delta_{m\,p})$ between the chemical shifts of para- and meta-fluorine atoms is strongly connected to the geometry at the boron centre and can be used to determine the strength of coordination of each R–OH compound [27]. The coordination strength at room temperature was shown to increase in the order Ph_3SiOH < (*c*-$C_5H_9)_7O_{12}Si_8(OH)$ < H_2O (Table 3). It can be noted that no or few HC_6F_5, resulting from $B\text{-}C_6F_5$ bond cleavage, was detected in the reaction mixture in our conditions.

^{11}B NMR spectra recorded after addition of R–OH to $B(C_6F_6)_3$ at room temperature showed single signals shifted upfield from the initial peak of free $B(C_6F_5)_3$ (Table 3). ^{11}B chemical shifts are also strongly dependent on the boron geometry and go upfield from trigonal to tetrahedral (neutral then anionic) structures. This confirmed the coordination of $B(C_6F_5)_3$ on the hydroxylic groups. The upfield shifts observed in ^{11}B NMR spectra of $B(C_6F_5)_3$ after reaction with R–OH

Table 3
^{1}H, ^{11}B and ^{19}F chemical shifts of $B(C_6F_5)_3$ before and after reaction with R–OH compounds

Solutions in C_6D_6				δ^1H (R–O*H*)			
	before	after	δ^{11}B	*o*-C_6F_5	*p*-C_6F_5	*m*-C_6F_5	$\Delta(\delta_{m,p})$
$B(C_6F_5)_3$	—	—	59	–128.7	–141.8	–160.1	18.3
$B(C_6F_5)_3 + Ph_3SiOH$	3.2	4.2	40	–130.4	–147.9	–161.0	13.1
$B(C_6F_5)_3 + (cC_5H_9)_7O_{12}Si_8(OH)$		5.2	27	–132.5	–152.0	–161.8	9.8
$B(C_6F_5)_3 + H_2O$		4.6	6.8	–134.8	–154.2	–163.0	8.8

increased in the order $Ph_3SiOH < (c\text{-}C_5H_9)_7O_{12}Si_8(OH) < H_2O$ (Table 3) and corroborated the coordination strengths evidenced by ^{19}F NMR spectroscopy.

We can then conclude from these studies that at the opposite of silanol groups, the molecular compounds R–OH [ROH = Ph_3SiOH, $(c\text{-}C_5H_9)_7O_{12}Si_8(OH)\cdot H_2O$] form a stable complex with $B(C_6F_5)_3$ (Eq. (5)).

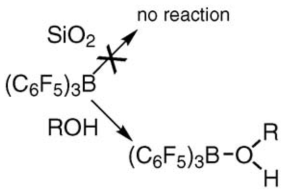

(5)

2.3. Reactivity of $B(C_6F_5)_3$ with silica surface in presence of a Brønsted base

The above results demonstrated that there was no interaction between $B(C_6F_5)_3$ and ≡Si–OH. At the opposite, pyridine forms hydrogen bonds with ≡Si–OH [28-30] (Eq. (6)). This hydrogen bond induces a higher negative charge on oxygen atom of ≡Si–OH, which could favour the formation of ion pair $[\equiv Si\text{–}O\,B(C_6F_5)_3]^-[HNC_5H_5]^+$. To verify this hypothesis, the reaction of toluene solution of C_5H_5N and $B(C_6F_5)_3$ (1:1) with SiO_2 was performed.

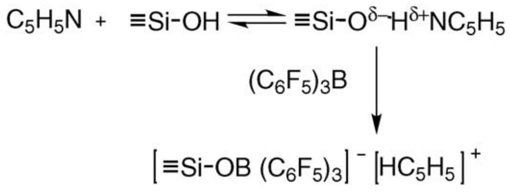

$$C_5H_5N + \equiv Si\text{-}OH \rightleftharpoons \equiv Si\text{-}O^{\delta-}H^{\delta+}NC_5H_5 \xrightarrow{(C_6F_5)_3B} [\equiv Si\text{-}OB\,(C_6F_5)_3]^-\,[HC_5H_5]^+ \quad (6)$$

2.3.1. Reactivity of **1** with pyridine

Pink silica pellets of **1** prepared by impregnation of $B(C_6F_5)_3$ on $SiO_{2-(500,700,1000)}$, were contacted with a vapour pressure of pyridine under static vacuum at room temperature. The ν(≡Si–OH) band at 3747 cm^{-1} due to free silanol disappeared and simultaneously a broad band resulting from hydrogen bonding between the surface silanols and pyridine appeared near 2900 cm^{-1}. Aromatic ν(C–H) and ν(C=C) vibrations were also observed at 3081, 3025, 3002 cm^{-1} and in the [1650–1500 cm^{-1}] region respectively, and were characteristic of the pyridine. The bands initially present at 1648 and 1523 cm^{-1} in **1** for the C_6F_5 groups were unaffected pyridine (respectively 1645 and 1519 cm^{-1} after desorption), while the strong one at 1483–1473 cm^{-1} was shifted by about 20 cm^{-1} to lower wavenumbers (1465 cm^{-1}). Other vibrations observed in **1** at 1394, 1383 and 1323 cm^{-1} disappear almost entirely after contact with pyridine. The same tendencies were noticed for the molecular compounds $B(C_6F_5)_3$ and $(C_6F_5)_3B.NC_5H_5$ adduct. The excess of pyridine was removed under vacuum (10^{-5} mbar) at room temperature. In the infrared spectra, the position of the peaks at 1632, 1492 and 1447 cm^{-1} indicates the presence of pyridine bonded to a Lewis acid site [28–30]. The shift of the peak of pyridine 8a mode [30] from 1583 to 1631 cm^{-1} ($\Delta\nu$ = 43 cm^{-1}) suggests the presence of strong strength Lewis acid. On the contrary, no bands at 1638, 1620 and 1540 cm^{-1}, characteristic of pyridine bonded to a Brønsted acid site on **1**, are observed (Fig. 3).

Solid-state ^{1}H NMR spectrum of **1** after reaction with $C_5H_5{}^{15}N$ shows a broad peak at 2.3 ppm, attributed to hydrogen-bound silanol groups, and three peaks at 7.4, 7.8 and 8.6 ppm characteristic of meta, para and ortho protons of the heterocycle. The solid state ^{15}N NMR spectra displayed a resonance at –150 ppm, characteristic of Lewis acidic site [26,30–34], unambiguously assigned to the Lewis acid-base

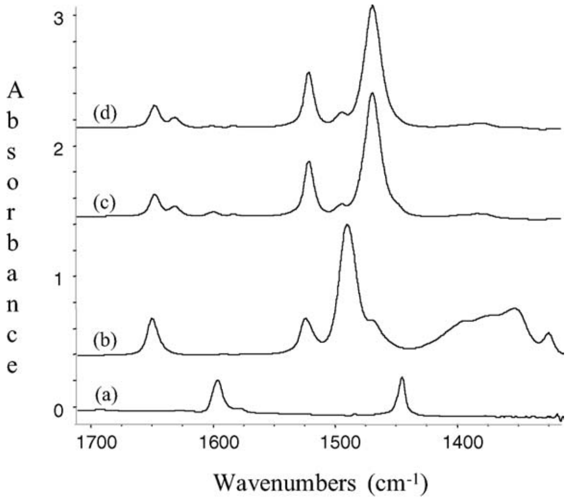

Fig. 3. IR spectra(silica spectra subtracted) of (**a**) $SiO_{2\text{-}(700)}$ + C_5H_5N; (**b**) $SiO_{2\text{-}(700)}$ after reaction with $B(C_6F_5)_3$ (5 equiv) in toluene; **1** (**c**) **1** + C_5H_5N (**d**) $(C_6F_5)_3B.NC_5H_5$/KBr; and expanded 1700–1400 cm^{-1} region.

adduct $(C_6F_5)_3B–NC_5H_5$, as demonstrated by comparison with the ^{15}N NMR spectrum of $(C_6F_5)_3B–(^{15}N\ C_5H_5)$ in the solid state (δ^{15}_N = –159.2 ppm). As by infrared studies, no Brønsted site acid was evidenced onto $B(C_6F_5)_3$-modified silica **1** by solid-state ^1H and ^{15}N NMR spectroscopies. The strong Lewis acidity detected on **1** is only due to homogeneous $(C_6F_5)_3B$-$(^{15}N\ C_5H_5)$ physisorbed on the surface. The reaction of $B(C_6F_5)_3$ and C_5H_5N (1:1) in toluene afforded quantitatively the complex $(C_6F_5)_3B.N\ C_5H_5$, **2**, which did not react with SiO_2, It was only physisorbed (Eq.(7)).

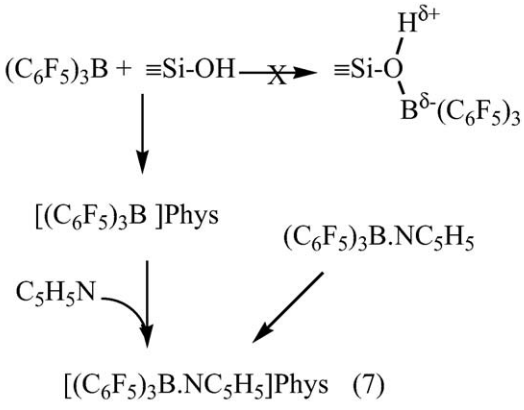

(7)

2.3.2. Reactivity of *1* with diethylaniline

The addition of one equivalent of NEt_2Ph to $B(C_6F_5)_3$ in aromatic solvents led instantaneously to a pink coloration of the solution, **S**. The stoichiometric reaction of $B(C_6F_5)_3$ and NEt_2Ph at room temperature, in an aromatic solvent, has been investigated by 1D and 2D NMR of ^1H,^{13}C, ^{11}B, ^{19}F and ^{15}N [35]. No adduct $Et_2PhN.B(C_6F_5)_3$ was formed. An equilibrium has been evidenced between free $(C_6F_5)_3B$ (40%) and Et_2NPh, imminium salt $(HB(C_6F_5)_3)^-(HNEt_2Ph)^+$ (30%), and zwitterionic stereoisomers *E* and *Z*-$[PhEtN^+{=}CH–CH_2B^-(C_6F_5)_3]$ in a 3:2 ratio (30%) [36]. In the presence of a protic compound, this equilibrium is totally displaced towards the ionic form $[RO–B(C_6F_5)_3]^-[HNEt_2Ph]^+$ [36].

Silica pellets **2** were prepared by impregnation of **S** on $SiO_{2–(300,500,800)}$. The IR band ascribed to isolated silanols at 3747 cm^{-1} disappeared totally and was replaced by broad bands at 3681, 3624 cm^{-1} (ν(OH) of interacting silanols) and by a sharp band at 3232 cm^{-1}. The intensity of the bands at 3681, 3624 cm^{-1} decreases inversely with the dehydroxylation temperature; simultaneously, that of the band at 3232 cm^{-1} increases (Fig. 4).

The use of labelled ^2H or ^{18}O silica proved that the band at 3232 cm^{-1} was due to a ν(N–H) vibration [36]. The structure of the supported species was confirmed by solid-state ^1H NMR [δC_6H_5 = 7.2, δCH_2 = 3.4, δCH_3 = 1 ppm], solid-state CP-MAS ^{13}C NMR [δCH_3 = 39, δCH_2 = 51 ppm] and solid-state ^{11}B NMR [δ = –8 ppm], in agreement with the ^{11}B chemical shift (solid state) of molecular analogous (–6.9 and –7 ppm), or literature data [6]. It is characteristic of an anionic borate fragment, i.e. $[≡SiO–B(C_6F_5)_3]^-$, in which the boron atom is tetracoordinated.

Elemental analyses of **2** /$SiO_{2–(300,500,700,800)}$ (Table 4) indicate a slight decrease in the weight percentage of boron, from 0.23 to 0.17%, when the dehydroxylation temperature of the silica is increasing from 300 to 800 °C. But no leaching of boron occurred after washing(see experimental part).

As demonstrated by infrared spectroscopy and elemental analysis, it must be emphasized that silanol groups could be only *partially* converted to ionic sites, depending on dehydroxylation temperatures. Indeed, weight percentages of boron corresponded to a proportion of modified silanols ranging from 37 to 96% when the pre-treatment temperatures of the silica increased from 300 to 800 °C.

In order to check if the experimental weight percentage of boron corresponded to the highest loading

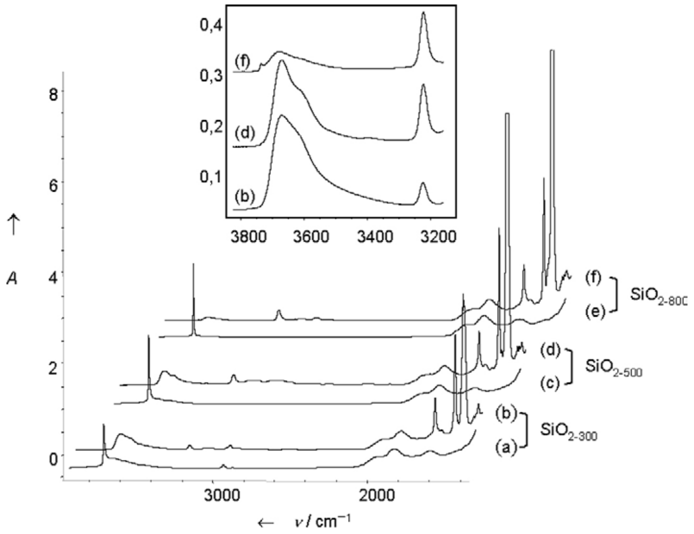

Fig. 4. IR spectra of (**a**) $SiO_{2-(300)}$; (**b**) $SiO_{2-(300)}$ after reaction with **S** (**S** = $B(C_6F_5)_3 + NEt_2Ph$, 1:1 mixture, 5 equivalents); (**c**) $SiO_{2-(500)}$; (**d**) $SiO_{2-(500)}$ after reaction with **S**; (**e**) $SiO_{2-(800)}$; (**f**) $SiO_{2-(800)}$ after reaction with **S**; and expended 3800–3200 cm^{-1} region.

Table 4
Elemental analysis of **2** in function of the dehydroxylation temperature of SiO_2

T (°C)	OH (nm^2)	%B [a]	%N [a]	B/N [b]	F/B [b,c]	C/(B+N) [b]	B/OH[d]	N/OH [d]
300	1.7	0.23	0.30	0.99	10.6	12.1	0.38	0.38
500	1.2	0.21	0.27	1.01	13.6	14.3	0.49	0.48
500	1.2	0.22	0.29	1	12	13	0.51	0.52
700	0.7	0.16	0.18	1.15	12.3	15.6	0.71	0.61
800	0.6	0.16	0.21	0.99	16.2	16.4	0.82	0.84
800	0.6	0.17	0.24	0.92	12.1	15.2	0.88	0.96
			Theory	1	15	14		

[a] Weight %.

[b] Molar ratios.

[c] Titration values obtained by conductimetry for fluorine in presence of boron were lowered by formation of BF_4^- anion.

[d] Calculated from respective weight percentages of boron and nitrogen.

achievable on the surface, modelling of **1** was performed using Sybyl computer modelling program. This entity was then grafted on a model of a partially dehydroxylated silica particle $SiO_{2-(500)}$ and minimized using the molecular mechanics Tripos force field [37–38]. A three-dimensional representation of the grafted model is depicted in (Fig. 5). The theoretical value obtained for the length of the B–O bond (1.567 Å) in the modelled complex was in the range of those reported for related silsesquioxane compounds (1.505–1.495 Å) [16,24–25]. The projected area of such a complex on the silica particle was estimated to 1.27 nm^2. According to the silica specific area (200 m^2 g^{-1}), this projection corresponds to a theoretical value of 0.24 w% of boron on a saturated surface. This result

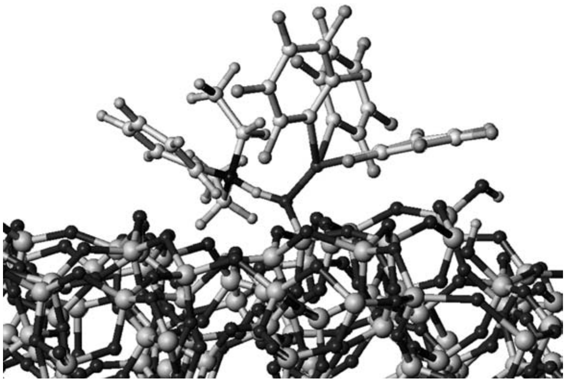

Fig. 5.

is in good agreement with the experimental percentages obtained on $SiO_{2-(500)}$ (0.21–0.22 w%).

Al spectroscopic and analytic data, as well as the similarities with those of molecular compounds $[HNEt_2Ph]^+[(C_6F_5)_3BOR]^-$ (R = H, $SiPh_3$, $Si_8O_{12}(c\text{-}C_5H_9)_7$) [17,36,39] confirmed the already proposed [6,7,9] structure for **2** (Eq. (8)).

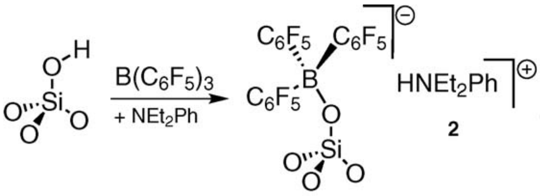

2 (8)

3. Conclusion

Infrared and solid-state ^1H NMR spectroscopies have shown that the dehydroxylation temperature can be used to understand and control the surface morphology of silica, e.g. the nature, distribution and concentration of reactive sites. It was shown that uniformity in surface reactive sites was only found for highly dehydroxylated silica surfaces (600–800 °C) as isolated silanols. At lower dehydroxylation temperatures ($T \leq 400$ °C), these latter coexist with H-bonded silanols. Moreover, the precise quantification of hydroxyl groups on silica allowed us to control subsequently the stoichiometry of surface reactions involved in the grafting of organometallic complexes.

Regarding the reaction of $B(C_6F_5)_3$ with silica surfaces, the coordination of the boron centre to a surface silanol group was not proved in the solid state. On the contrary, infrared and solid-state ^1H and ^{11}B NMR studies showed that the silanol groups were not affected by the presence of $B(C_6F_5)_3$ on silica surface, and that the boron atom has kept a trigonal planar configuration. As no or few HC_6F_5 was detected in the impregnation solutions, the cleavage of B–C bounds by surface silanols was ruled out as a major reaction pathway. $B(C_6F_5)_3$ was only physisorbed onto the silica surface.

In the presence of the strongly nucleophilic pyridine, the formation of the adsorbed Lewis acid-base adduct, $(C_6F_5)_3B.NC_5H_5$, was privileged, displaced the reaction (6) totally towards the right. Such a reaction was also described for homogeneous silsesquioxane models.

The interaction of $B(C_6F_5)_3$ with silica in the presence of Et_2NPh yielded to $[\equiv Si–O–B(C_6F_5)_3]^-[HNEt_2Ph]^+$. The formation of $[\equiv Si–O–B(C_6F_5)_3]^-[HNEt_2Ph]^+$is probably due to the nature of NEt_2Ph which cannot, due to the steric congestion (B-strain), form a complex with $B(C_6F_5)_3$, at the opposite of pyridine and Me_2NPh [36]. The use of the stoichiometric nature of surface organometallic chemistry allowed us to transform selectively each surface silanol group [≡SiOH] into a *unique* and well-defined ionic entity $[\equiv SiO–B(C_6F_5)_3]^-[HNEt_2Ph]^+$ only when the pretreatment temperature of the silica was 800 °C and above. Out of these conditions, on the silica surface, two types of surface sites were found: the free silanol groups [≡SiOH] and the ionic $[\equiv SiO–B(C_6F_5)_3]^-[HNEt_2Ph]^+$ groups in relative proportion of 3:2 for $SiO_{2-(300)}$ and 1:1 for $SiO_{2-(500)}$. This surface $[\equiv SiO–B(C_6F_5)_3]^-[HNEt_2Ph]^+$ is the first example of the selective preparation and full characterization of a heterogeneous non-coordinating anion/free cation system. This surface fragment can be used as a very promising building block to generate cationic heterogeneous anions on which the metallocenium species are stabilized by ion-pair interactions. Accordingly, the reaction of Cp^*ZrMe_3 with $[\equiv SiO–B(C_6F_5)_3]^-[HNEt_2Ph]^+$, afforded, by an irreversible process of methane elimination, to an unique and well-defined cationic silica-supported metallocenium species $[\equiv SiO–B(C_6F_5)_3]^-[Cp^*ZrMe_2(NEt_2Ph)]^+$, which was an active olefin polymerisation catalyst [41].

4. Experimental

4.1. General procedures

Solid-state NMR spectra were recorded on a Bruker DSX-300 spectrometer equipped with a standard 4-mm double-bearing probe head and operating at 75.47, 96.31, 30.43, and 300.18 MHz for ^{13}C, ^{11}B, ^{15}N and ^1H, respectively. Chemical shifts were given with respect to external references (^1H, ^{13}C, TMS at 0 ppm; ^{11}B, $BF_3.OEt_2$ at 0 ppm; ^{15}N, CH_3NO_2 at 0 ppm). The samples were introduced in the zirconia rotor in a glovebox and tightly closed. Solution NMR spectra were recorded on Bruker AC 200 MHz (^{19}F), AC 300 MHz (^1H, ^{13}C), DRX 300 MHz (^{11}B) and DRX 500 MHz (^1H, ^{13}C, ^{11}B, ^{15}N) spectrometers. Chemical shifts were reported in ppm and referenced to residual solvent resonances (C_6D_6: 7.15 for ^1H, 128 for ^{13}C; CD_2Cl_2: 5.32 for ^1H, 53.8 for ^{13}C), or external standards (^{19}F, $CFCl_3$ at 0; ^{11}B, $BF_3.OEt_2$ at 0; ^{15}N, CH_3NO_2 at 0). Infrared spectra were recorded under vacuum on a Nicolet 550 FT spectrometer by using an infrared cell equipped with CaF_2 windows, allowing in situ studies. Typically, 16 scans were accumulated for each spectrum. KBR pellets were prepared for molecular compounds. Elemental analyses were performed by the Central Analysis Service of the CNRS at Solaize.

All operations were performed in the strict absence of oxygen and water under a purified argon atmosphere using glovebox (Jacomex or MBraun) or vacuum-line techniques. Toluene and pentane were distilled under argon from Na/K alloy, degassed and stored under argon over Na (toluene) or 3–Å molecular sieves (pentane). C_6D_6 (SDS – 99.6%) and CD_2Cl_2 (SDS – 99.6%) were degassed by three cycles of 'freeze-pump-thaw' and dried over freshly regenerated 3 Å molecular sieves. Pyridine (Aldrich, 99%) was dried on solid KOH and distilled under argon, degassed and stored over 3–Å molecular sieves. Labelled ^{15}N pyridine (Aldrich, 99%) was degassed and store over 3Å molecular sieves. $B(C_6F_5)_3$ (Merck Chemicals, > 97%) was dried on Me_3SiCl [40], purified by vacuum sublimation and its purity was checked by ^{19}F NMR before using. The 3,5,7,9,11,13,15-heptacyclopentyl-pentacyclooctasiloxan-1-ol and the triphenylsilanol were purchased from Aldrich Chemical and dried under vacuum before use. The synthesis of $B(C_6F_5)_3.OH_2$ [13] [16], $B(C_6F_5)_3.N\,C_5H_5$ [17], and $[Z\text{–}O\,B(C_6F_5)_3]^-$ $[HNEt_2Ph]^+$ with Z–OH, Z = H, Ph_3Si, $(c\text{-}C_5H_9)_7O_{12}Si_8$ [36], or silica were performed according to literature procedures. Silica support (Aerosil® Degussa, 200 $m^2\,g^{-1}$) was compacted to a disk (30 mg) for infrared studies or was hydrated, dried (80 °C) and crushed to prepare large quantities (1–2 g) for NMR studies and elemental analyses. Before reaction, to prepare large quantities, silica was calcinated at 400 °C in air for 4 h, and dehydroxylated at the desired temperature (500, 700, 800 or 1000 °C) under high vacuum (10^{-5} Torr) for 12 h (referred respectively as $SiO_{2\text{–}(500)}$, $SiO_{2\text{–}(700)}$ and $SiO_{2\text{–}(1000)}$), except in the case of silica dehydroxylated at 300 °C (referred as $SiO_{2\text{–}(300)}$), which was calcinated at 400°C in air for 4 h, rehydrated with distilled water and then dehydroxylated at 300 °C for 12 h. The surface areas were measured by N_2 adsorption and treatment of data using BET method.

4.2. Preparation of the $B(C_6F_5)_3$-modified silica supports, *1*, and reactivity with pyridine

4.2.1. For infrared experiments

A disk of compacted $SiO_{2\text{–}(700)}$ (30 mg) was reacted under argon and at room temperature with a solution of 16 mg (0.031 mmol, 5 equiv) of $B(C_6F_5)_3$ in 10 ml of toluene during 2–3 h. The pink pellet was then washed with three fractions of 10 ml of dry toluene and dried 1 h at room temperature under 10^{-5} mbar. IR spectra were recorded before and after washings. IR (cm^{-1}): 3748 (s) $\nu(O\text{–}H)_{isolated}$, 1650 (m) C_6F_5, 1523 (m) C_6F_5, 1491 (s) C_6F_5, 1470 (m) C_6F_5, 1395 (m), 1380 (m) C_6F_5, 1354 (m), 1325 (m). The same procedure was used for $SiO_{2\text{–}(500)}$ and $SiO_{2\text{–}(1000)}$.

4.2.2. For large-scale preparation (NMR and elemental analysis samples)

A solution of 107 mg (0.21 mmol–1 equiv) of $B(C_6F_5)_3$ in 10 ml of dry toluene was filtered under argon onto 1 g of compacted $SiO_{2\text{–}(700)}$. The pink suspension was stirred under argon for 1–2 h at room temperature. The colourless impregnation solution was then either evaporated to give $\mathbf{1}_e$, or filtered, removed with a syringe and the solid washed three times with 10 ml of dry toluene to give $\mathbf{1}_w$. The pink solids $\mathbf{1}_e$ and $\mathbf{1}_w$ were finally dried under vacuum (10^{-5} mbar) for 4 h at room temperature. Elemental analysis: w% B = 0.13. $\mathbf{1}_e$, $\mathbf{1}_w$: solid-state ^1H NMR (δ): 2.1 (s, isolated ≡Si–OH). No peak detected in solid-state ^{11}B NMR spectra. The same procedures were used for $SiO_{2\text{–}(300)}$ and $SiO_{2\text{–}(500)}$ and similar results were obtained.

4.3. Adsorption of pyridine on *1*

4.3.1. For infrared experiments

A vapour pressure of pyridine was condensed at 73 K onto $B(C_6F_5)_3$-impregnated silica pellets **1** (30 mg) prepared as described above. After warming to room temperature, the colour of the solid changed from pink to white. The excess of pyridine was then desorbed under vacuum (10^{-5} mbar) during 1 h at room temperature. Infrared spectra were recorded at various desorption times and at room temperature. IR (cm^{-1}):

3747 (s) ν(O–H)$_{\text{isolated}}$, 1646 (m) C_6F_5, 1631 (m) L-bonded C_5H_5N, 1599 (m) H-bonded C_5H_5N, 1583 (w) physisorbed C_5H_5N, 1520 (m) C_6F_5, 1492 (w) L+H-bonded C_5H_5N, 1469 (s) C_6F_5, 1446 (w) L+H-bonded C_5H_5N, 1396 (w) C_6F_5, 1384 (w) C_6F_5.

4.3.2. For larger scale preparation (NMR and elemental analysis samples)

Same procedure with a vapour pressure of labelled ^{15}N pyridine onto 100 mg of $B(C_6F_5)_3$-impregnated silica $\mathbf{1_e}$ and $\mathbf{1_w}$. After reaction with pyridine (^{15}N), the colour of the solids changed from pink to white at room temperature. $\mathbf{1_w}$: Solid-state ^{1}H NMR (δ): 2.2 (br.s, H-bonded ≡Si–OH), 7.4 (s, *m*-C_5H_5N), 7.8 (s, *p*-C_5H_5N), 8.5 (s, *o*-C_5H_5N). Solid-state ^{15}N NMR (δ): –106 (s, Lewis acidic centre), ε –153 (s, $(C_6F_5)_3B{\cdot}NC_5H_5$). No peak observed in ^{11}B NMR spectra. $\mathbf{1_e}$: solid-state ^{1}H NMR (δ): 8.2 (br.s, C_5H_5N), 1.9 (s, ≡SiOH). Solid-state ^{15}N NMR (δ): –102 (s, Lewis acidic centre), –160 (s, $C_6F_5)_3B{\cdot}NC_5H_5$). Solid-state ^{11}B NMR (δ): –7.6 (s, $C_6F_5)_3B.NC_5H_5$), –11.8 (s).

4.4. Reactivity of $B(C_6F_5)_3$ with H_2O

Addition of 7 µl (0.39 mmol) of distilled water to a solution of 206 mg (0.4 mmol, 1 equiv) of $B(C_6F_5)_3$ in 12 ml of pentane led to precipitation of a white solid. The suspension was stirred overnight, and the crude product obtained after filtration was washed three times with pentane (4 ml) and dried 1 h under vacuum. Yield (175 mg, 82%) ^{1}H NMR (C_6D_6, δ): 4.6 (s, OH). ^{13}C NMR (C_6D_6, δ): 148.0 (d, $^1J_{C–F}$ = 242 Hz, *o*-C_6F_5), 141.5 (d, $^1J_{C–F}$ = 254 Hz, *p*-C_6F_5), 137.6 (d, $^1J_{C–F}$ = 255 Hz, *m*-C_6F_5), 114.6 (br.s, *i*-C_6F_5). ^{19}F NMR (C_6D_6, δ): –134.8 (d, $^3J_{F–F}$ = 23 Hz, 6F, *o*-C_6F_5), –154.3 (t, $^3J_{F–F}$ = 21 Hz, 3F, *m*-C_6F_5), –162.5 (t, $^3J_{F–F}$ = 23 Hz, 6F, *m*-C_6F_5). ^{11}B NMR (C_6D_6, δ): 6.8 (s, $(C_6F_5)_3B–OH_2$). IR (KBr, cm^{-1}): 3565 (m), 3502 (m), 1652 (m), 1610 (w), 1523 (s), 1473 (s), 1382 (m), 1292 (m), 1270 (w), 1246 (w), 1122 (m), 1112 (m), 1093 (m), 1014 (w), 974 (s).

4.5. Reactivity of $B(C_6F_5)_3$ with Ph_3SiOH

In a NMR tube, 75 mg (0.15 mmol – 1 equiv) of $B(C_6F_5)_3$ was added at room temperature to a solution of 40 mg (0.14 mmol) of Ph_3SiOH in 0.5 ml of *d$_6$*-benzene. A clear colourless solution was obtained after stirring. ^{1}H NMR (C_6D_6, δ): 7.5 (d, $^3J_{H–H}$ = 7.5 Hz, 6H, *o*-C_6H_5), 7.1 (*m*, 9H, *p*- and *m*-C_6H_5), 4.2 (br.s, 1H, –OH). ^{13}C NMR (C_6D_6, δ): 148.2 (d, $^1J_{C–F}$ = 244 Hz, *o*-C_6F_5), 137.7 (d, $^1J_{C–F}$ = 255 Hz, *m*-C_6F_5), 135.6 (s, *o*-C_6H_5), 133.1 (s, *i*-C_6H_5), 131.0 (s, *p*-C_6H_5), 128.4 (s, *m*-C_6H_5), *p*- and *i*-C_6F_5 carbons non resolved. ^{19}F NMR (C_6D_6, δ): –130.4 (d, $^3J_{F–F}$ = 17 Hz, 6F, *o*-C_6F_5), –147.9 (br.s, 3F, *p*-C_6F_5), –161.0 (*m*, 6F, *m*-C_6F_5). ^{11}B NMR (C_6D_6, δ): 40 (br.s, $Ph_3Si(OH)B(C_6F_5)_3$).

4.6. Reactivity of $B(C_6F_5)_3$ with $(c\text{-}C_5H_9)_7O_{12}Si_8(OH)$

In a NMR tube, 75 mg (0.15 mmol, 1 equiv) of $B(C_6F_5)_3$ was added at room temperature to a solution of 135 mg (0.15 mmol) of $(c\text{-}C_5H_9)_7O_{12}Si_8(OH)$ in 0.5 ml of *d$_6$*-benzene. A clear colourless solution was obtained after stirring. ^{1}H NMR (C_6D_6, δ): 5.2 (br.s, 1H, OH), 1.8 (m, 14H, CH_2 C_5H_9), 1.6 (m, 28H, CH_2 C_5H_9), 1.4 (m, 14H, CH_2 C_5H_9), 1.1 (m, 7H, CH C_5H_9). ^{13}C {^{1}H} NMR (C_6D_6, δ): 148.4 (d, $^1J_{C–F}$ = 240 Hz, *o*-C_6F_5), 141.9 (d, $^1J_{C–F}$ = 254 Hz, *p*-C_6F_5), 137.6 (d, $^1J_{C–F}$ = 253 Hz, *m*-C_6F_5), 27.7, 27.6, 27.5, 27.4, 27.3 (s, CH_2 C_5H_9), 22.5, 22.3, 21.9 (s, CH C_5H_9). ^{19}F NMR (C_6D_6, δ): –132.6 (br.s, 6H, *o*-C_6F_5), –152.0 (br.s, 3H, *p*-C_6F_5), –161.8 (m, 6H, *m*-C_6F_5). ^{11}B NMR (C_6D_6, δ): 27 (br.s, $(c\text{-}C_5H_9)_7O_{12}Si_8(OH)B(C_6F_5)_3$).

4.7. Preparation of $(C_6F_5)_3B–NC_5H_5$

To a solution of 0.248 g (0.48 mmol) of $B(C_6F_5)_3$ in 5 ml of toluene was added 0.042 ml (0.52 mmol) of pyridine to give a colourless solution. After stirring for 1 h, the toluene was evaporated under vacuum to leave a white solid which was washed twice with pentane (2 ml) and dried for 1 h at room temperature. Yield = 0.234 g (0.40 mmol – 82%). ^{1}H NMR (C_6D_6, δ): 7.94 (d, $^3J_{H–H}$ = 5 Hz, 2H, *o*-C_5H_5N), 6.57 (t, $^3J_{H–H}$ = 7 Hz, 1H, *p*-C_5H_5N), 6.24 (t, $^3J_{H–H}$ = 7 Hz, 2H, *m*-C_5H_5N). ^{13}C {^{1}H} NMR (C_6D_6, δ): 148.3 (d, $^1J_{C–F}$ = 243 Hz, *o*-C_6F_5), 146.4 (s, *o*-C_5H_5N), 141.7 (s, *p*-C_5H_5N), 140.8 (d, $^1J_{C–F}$ = 232 Hz, *p*-C_6F_5), 137.7 (d, $^1J_{C–F}$ = 242 Hz, *m*-C_6F_5), 124.9 (s, *o*-C_5H_5N), 118.6 (br.s, *i*-C_6F_5). ^{19}F NMR (C_6D_6, δ): –131.4 (d, $^3J_{F–F}$ = 21 Hz, 6F, *o*-C_6F_5), –155.4 (t, $^3J_{F–F}$ = 21 Hz, 3F, *p*-C_6F_5), –162.6 (t, $^3J_{F–F}$ = 19 Hz, 6F, *m*-C_6F_5). ^{11}B

NMR (C_6D_6, δ): –3.7 (s, $(C_6F_5)_3B–NC_5H_5$). ^{15}N NMR (C_6D_6, δ): –158.2 (s, $(C_6F_5)_3B–NC_5H_5$). IR (KBr, cm^{-1}): 1646 (m) C_6F_5, 1631 (m) L-bonded C_5H_5N, 1578 (w) C_5H_5N, 1520 (s) C_6F_5, 1495 (m) L-bonded C_5H_5N, 1462 (vs) C_6F_5, 1385 (m) C_6F_5, 1378 (m) C_6F_5, 1293 (m), 1283 (m), 1252 (m), 1242 (m), 1224 (m), 1162 (w), 1115 (m), 1098 (m), 1028 (w), 991 (s) C_6F_5, 981 (s) C_6F_5, 962 (m) C_6F_5.

References

[1] W. Kaminsky (Ed.), Metalorganic Catalysts for Synthesis and Polymerization: Recent Results by Ziegler–Natta and Metallocene Investigations, Springer-Verlag, Berlin, 1999.

[2] E.Y.-X. Chen, T.J. Marks, Chem. Rev. 100 (2000) 1391.

[3] G.G. Hlatky, Chem. Rev. 100 (2000) 1347.

[4] C. Coperet, M. Chabanas, R. Petroff Saint-Arroman, J.-M. Basset, Angew. Chem. Int. Ed. Engl. 42 (2003) 156.

[5] A.G. Massey, A.J. Park, F.G.A. Stone, Proc. Chem. Soc. (1963) 212.

[6] J. Walzer, J. Flexer, in: US Patent 5 643 847, Exxon Chemicals, 1997.

[7] D.G. Ward, E.M. Carnahan, in: US Patent 5 939 347, W.R. Grace and Co., 1999.

[8] J. Tian, S. Wang, Y. Feng, J. Li, S. Collins, J. Mol. Catal. 144 (1999) 137.

[9] M. Bochmann, G.J. Pindado, S.J. Lancaster, J. Mol. Catal. 146 (1999) 179.

[10] S.J. Lancaster, S.M. O'Hara, M. Bochmann, in: W. Kaminsky (Ed.), Metalorganic Catalysts for Synthesis and Polymerization, Springer, 1999.

[11] A.R. Siedle, W.M. Lamanna, R.A. Newmark, Makromol. Chem., Macromol. Symp. 66 (1993) 215.

[12] A.R. Siedle, W.M. Lamanna, in: US Patent 5 296 433, 3M Company, 1994.

[13] D.C. Bradley, I.S. Harding, A.D. Keefe, M. Motevalli, D.H. Zheng, J. Chem. Soc., Dalton Trans. (1996) 3931.

[14] A.A. Danopoulos, J.R. Galsworthy, M.L.H. Green, S. Cafferkey, L.H. Doerrer, M.B. Hursthouse, Chem. Commun. (1998) 2529.

[15] L.H. Doerrer, M.L.H. Green, J. Chem. Soc., Dalton Trans. (1999) 4325.

[16] C. Bergquist, B.M. Bridgewater, C.J. Harlan, J.R. Norton, R.A. Friesner, G. Parkin, J. Am. Chem. Soc. 122 (2000) 10581.

[17] (a) R. Duchateau, R.A. Van Santen, G.P.A. Yap, Organometallics 19 (2000) 809; (b) R. Duchateau, Chem. Rev. 102 (2002) 3525–3542.

[18] R.K. Iler, The Chemistry of Silica, John Wiley & Sons, New York, 1979.

[19] B.A. Morrow, A.J. McFarlan, J. Non-Cryst. Solids 120 (1990) 61.

[20] E.F. Vansant, P. Van Der Voort, K.C. Vrancken, Characterization and chemical modification of the silica surface, 95, Elsevier, Amsterdam, 1995.

[21] G.E. Maciel, D.W. Sindorf, J. Am. Chem. Soc. 102 (1980) 7607.

[22] D.W. Sindorf, G.E. Maciel, J. Am. Chem. Soc. 105 (1983) 1487.

[23] C.A. Fyle, G.C. Gobbi, G.J. Kennedy, J. Phys. Chem. 89 (1985) 277.

[24] A.G. Massey, A.J. Park, J. Organomet. Chem. 2 (1964) 245.

[25] R.D. Chambers, T. Chivers, Organomet. Chem. Rev. 1 (1966) 279.

[26] J. Zhang, J.B. Nicholas, J.F. Haw, Angew. Chem. Int. Ed. Engl. 39 (2000) 3302.

[27] A.D. Horton, J. de With, A.J. Van der Linden, H. Van de Weg, Organometallics 15 (1996) 2672.

[28] G. Buscha, Catal. Today 41 (1998) 191 and references therein.

[29] L. Ferratto, A. Glisenti, J. Mol. Catal. 187 (2002) 119.

[30] E.P. Parry, J. Catal. 2 (1963) 371.

[31] G.E. Maciel, J.F. Haw, I.S. Chuang, B.L. Hawkins, T.A. Early, D.R. McKay, L. Petrakis, J. Am. Chem. Soc. 105 (1983) 5529.

[32] R.O. Duthaler, J.D. Roberts, J. Am. Chem. Soc. 100 (1978) 4969.

[33] J.A. Ripmeester, J. Am. Chem. Soc. 105 (1983) 2925.

[34] J.F. Haw, I.S. Chuang, B.L. Hawkins, G.E. Maciel, J. Am. Chem. Soc. 105 (1983) 7206.

[35] N. Millot, C.C. Santini, B. Fenet, J.-M. Basset, Eur. J. Inorg. Chem (2002) 3328.

[36] N. Millot, A. Cox, C.C. Santini, Y. Mollard, J.-M. Basset, Chem. Eur. J. (2002) 1438.

[37] M. Clark, R.D. Cramer III, Van Opdenbosh, J. Comput. Chem. 10 (1989) 982.

[38] J.J.P. Steward, J. Comput. Chem. 10 (1991) 320.

[39] A.R. Siedle, R.A. Newmark, W.M. Lamanna, J.C. Huffman, Organometallics 12 (1993) 1491.

[40] L.W.M. Lee, W.E. Piers, M. Parvez, S.J. Rettig, V.G. Young, Organometallics 18 (1999) 3904.

[41] N. Millot, C.C. Santini, A. Baudouin, J.-M. Basset, Chem. Commun. (2003) 2034.